SENSOR PROPERTIES OF HETEROCYCLIC COMPOUND WITH DOPED NANOPARTICLES

A. Mathunika Devi[1], J. Lesy Josephine[2,3], P. Ramanathan[1*], K. Thanigaimani[2], M. Suresh[4]

Abstract

Quenching and enhancing behaviour of 1-(4-methoxyphenyl)-2-(4-methylnaphthalen-1-yl)-1H-phenanthro[9,10-d] imidazole (Ligand - MMPI) with Cu –doped ZnO nanoparticle has been studied. Ligand has been characterized by ^{1}H, ^{13}C NMR and mass spectral analysis. Cu –doped ZnO nanoparticle have been synthesised by sol-gel method and characterized by powder X-ray diffraction (XRD), Scanning Electron Microscope (SEM) and Energy Dispersive X-ray Spectra (EDS). Quenching and enhancing behaviour were confirmed by the ligand strongly binding on the surface of Cu –doped ZnO nanoparticle. Increasing concentration of nanoparticles into ligand results in enhances absorbance and quenching fluorescence was observed. Fluorescence quenching was confirmed electron transfer from excited state of ligand to nanoparticle. Theoretical calculations were performed by Gaussian -03 package.

Keywords: Ligand; Cu –doped ZnO; XRD, SEM, EDS

[1*]PG & Research Department of Chemistry, Thanthai Hans Roever College (Autonomous), (Affiliated to Bharathidasan University), Perambalur - 621220, Tamilnadu, India
[2]PG & Research Department of Chemistry, Government Arts College, (Affiliated to Bharathidasan University), Tiruchirappalli – 620 022, Tamilnadu, India
[3]Department of Chemistry, Immaculate College for Women, (Affiliated to Annamalai University), Cuddalore – 607 006, Tamilnadu, India.
[4]PG & Research Department of Chemistry, AVS College of Arts and Science (Autonomous), (Affiliated to Periyar University), Ramalingapuram - 636106, Tamilnadu, India

***Corresponding Author:** P. Ramanathan
*PG & Research Department of Chemistry, Thanthai Hans Roever College (Autonomous), (Affiliated to Bharathidasan University), Perambalur - 621220, Tamilnadu, India, Email: ramanathanp2010@gmail.com

DOI: 10.31838/ecb/2023.12.5.484

1. Introduction

Tunable multicolour emissions natured materials have arriving significant notice for their opto-electronics as prospective light emitting displays [1] and biological characterisation [2]. There are three kinds of materials are used to construct multicolour emission [3-7], they are organic dye-doped semiconducting polymer nanoparticles, quantum dots of different sizes and lanthanide-doped, nanomaterials. A wide band gap of 3.37 eV (at 300 K) is gained by ZnO, it is vital II-VI semiconductor and due to electron hole recombination it emits illumination in the range of 375–405 nm. Because of defect or trapped states it gives green emission at 545 nm. Due to alone ionized oxygen position in the ZnO nanocrystals the green emission is originated. Because of its nontoxicity and chemical stability the great consideration for bio-imaging applications is achieved by ZnO nanocrystals. Effectively tuned from blue to yellow [8, 9] is by the emission of nanostructured ZnO. Yellow emission is very bright compared to blue emission. Blue emission of the ZnO nanosemiconductor has not been better projection in biological labelling as compared to the green and yellow emissions. Applications for these new classes of materials have been inspired for some intensive investigations. Variety of materials like cerium, zinc, and iron oxides, titanium can be composed of metal oxide nanoparticles [10]. The yielding is entirely new and different physico-chemical properties as there are changes in their fundamental physical and chemical and properties causes a major change in the size of such particle. These particles widely used for gas sensors, non-linear optics, catalysis, cosmetics varistors, pigments, solar energy exchange, etc. [11-14]. ZnO has been calculated in transparent UV protection films, transparent conductors, chemical sensors and varistors and so on as a large band gap semiconductor [15,16]. The report as Xia et al is for Polymer-stabilized nano ZnO with blue emission [17] and the cell imaging is obtained by tunable photoluminescence with

and the ZnO@polymer core–shell nanoparticles [18,19]. Using single crystals or polycrystalline of Co^{2+} : ZnO prepared by pellet sintering many scholars identified the visible photo-response of Co-doped ZnO. They found that the nickel-doped ZnO hollow spheres exhibited only weak ferromagnetism at 300 K whereas Co-doped ZnO hollow exhibited ferromagnetism at room temperature. Not due to any cobalt oxide phase formation or any metallic Co segregation the observed nature of ferromagnetism was intrinsic. By Tao Liu et al., Herein about 5 nm in size the Co-doped ZnO nanoparticles were synthesized and we report the binding interaction and surface behaviour of ZnO nanoparticles by MMPI, results by the spectral studies were unexpected unfortunately. Fluorescence quenching results which is obtained is an unique study of interaction between Cu -doped ZnO and 1-(4-methoxyphenyl) -2-(4-methylnaphthalen-1-yl)-1H-phenanthro [9,10-d] imidazole.

2. Experimental

2.1. Synthesis of 1-(4-methoxyphenyl)-2-(4-methylnaphthalen-1-yl)-1H-phenanthro [9,10-d]imidazole

4-methyl-1-naphthaldehyde (1 mmol), phenanthrene-9,10-dione(1mmol),4- methoxyaniline (1 mmol) and NH_4OAc (1mmol) with borontrifluride ethyletharate (1 mol%) as catalyst was stirred at 80 °C for 2 hrs. The movement of the reaction was monitored by TLC (Scheme 1). After end of the reaction the mixture was cooled, dissolved in dichloromethane and filtered. The product was purified by column chromatography using benzene: hexane (9:1) as the eluent. ^{1}H NMR (400 MHz, DMSO): δ 2.32 (s, 3H), 3.72 (s, 3H), 8.94 (d, J = 8.4 Hz, 1H), 8.91 (d, J = 8.4 Hz, 1H), 8.68 (d, J = 7.6 Hz, 1H), 7.88 (d, J = 8.0 Hz, 1H), 7.76 (d, J = 7.2 Hz, 1H), 7.56 (d, J = 7.6 Hz, 1H), 7.39 (t, 1H), 7.21 (d, J = 8.0 Hz, 1H), 6.95 (d, J = 8.4 Hz, 2H), 7.97 (t, 2H), 7.68 (t, 2H), 7.55-7.42 (m, 5H). ^{13}C NMR (400 MHz, DMSO): δ 21.31, 55.28, 114.62, 120.27, 121.98, 122.59, 123.66, 124.42, 124.67, 125.19, 125.60, 125.78, 126.20, 126.69, 126.82, 126.86, 127.24, 127.42, 127.64, 128.04, 128.09, 128.29, 128.41, 129.50, 129.52, 129.72, 129.95, 132.35, 132.76, 136.28, 150.47, 159.47. m/z. 464.56 [M+].

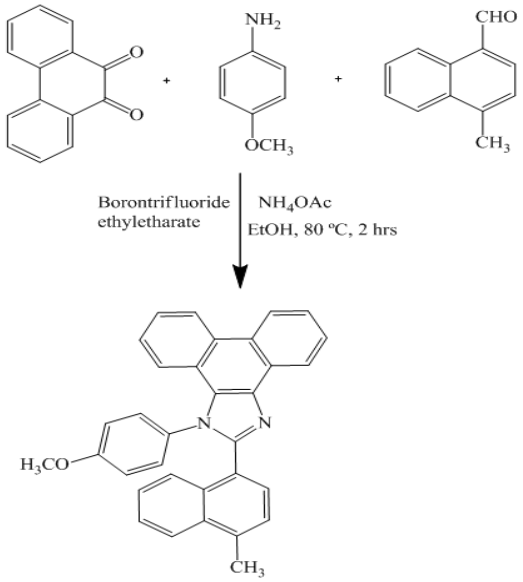

Scheme 1. Synthetic route of 1-(4-methoxyphenyl)-2-(4-methylnaphthalen-1-yl)-1H-phenanthro[9,10-d]imidazole

2.2. Synthesis of Cu-doped ZnO by Sol-gel method

To the zinc acetate (0.1g) solution with copper nitrate in 10ml 0.01 M polyvinyl pyrrolidone K-30, freshly prepared solution of 1:1 aq. ammonia was added slowly to reach a pH of 7, under constant stirring. The stirring was continued for another 30 minutes to get a gel. The formed glassy like white gel was permitted to overnight. It was filtered and washed with water a number of times, dried at 100 °C for 1 hrs and calcinated at 400 °C for 3 hrs to pale grey solid.

2.3. Measurements

The ^{1}H and ^{13}C NMR spectra at 400 and 100 MHz, respectively were obtained at room temperature using a Bruker 400 MHz NMR spectrometer (Bruker biospin, California, USA). XRD patterns were recorded for the centrifuged and dried samples using X–ray Rigaku diffractometer with Cu K_α source (30 kV, 100 mA), at a scan speed of 3.0000 deg/min, step width of 0.1000 deg, in a 2θ range of 20-80°. The energy dispersive X-ray (EDS) spectra of the nanosemiconductors were recorded with a JEOL JSM-5610 scanning electron microscope (SEM) equipped with back electron (BE) detector and EDX. The sample was placed on an adhesive carbon slice supported on copper stubs and coated with 10 nm thick gold using JEOL JFC- 1600 auto fine coater prior to measurement. The binding relations of ligand with nanoparticles has been recorded using UV–vis spectroscopy by employing a Systronics Double beam UV–vis spectrophotometer operated on 200–800 nm wavelengths. The fluorescence measurements have been carried out with a Perkin Elmer LS45

spectrofluorimeter. DFT calculations were performed with Gaussian-03 [20] package.

3. Results and discussion

3.1. XRD and SEM analysis Cu -doped ZnO nanoparticle

X-ray diffraction pattern (XRD) of (Figure 1) Cu -doped ZnO nanoparticle obtained by sol-gel method. The diffraction patterns match with the standard JCPDS card number (89-7102). The crystal structure of Cu -doped ZnO are primitive hexagonal with crystal constants a and b as 3.253 Å and c as 5.029 Å. In the case of doping with copper, as the radii of Zn^{2+} and Cu^{2+} are similar, Cu^{2+} can change Zn^{2+} in the pattern without vary in the pattern parameters. The XRD of Cu -doped ZnO fails to present any peak other than those of ZnO. The average crystallite sizes (L) of the sol–gel synthesized Cu- doped ZnO have been deduce as 25 nm, respectively. They have been obtained from the full width at half maximum (FWHM) of the most intense peaks of the individual crystals by the Scherrer equation, $L = 0.9\ \lambda/\beta\cos\theta$, where λ is the wavelength of the X-rays used, θ is the diffraction angle and β is the full width at half maximum of the peak. Calculated surface area for Cu- doped ZnO is 39.54 m^2/g. The scanning electron micrographs (SEM) of Cu -doped ZnO nanoparticle are shown in figure 2. The EDS spectra are shown in figure 3, presence of zinc, oxygen, copper signals confirms the purity of the synthesized Cu –doped ZnO nanoparticle.

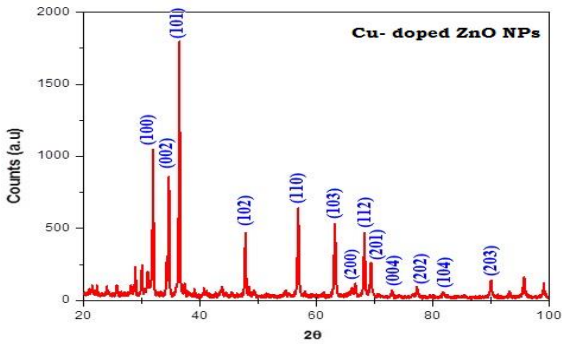

Fig 1. X-ray diffraction pattern of (XRD) of Cu-doped ZnO nanoparticle

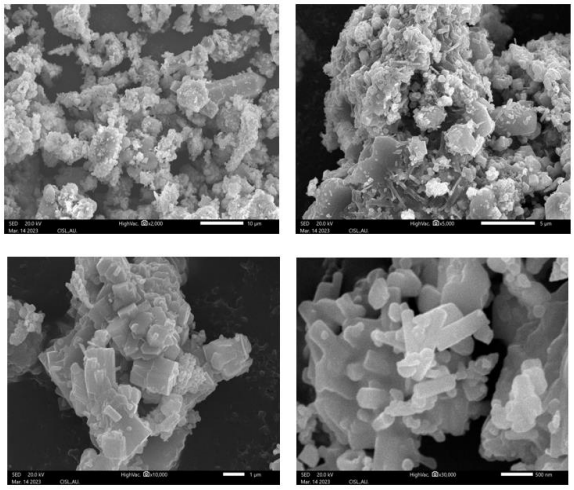

Fig. 2. SEM images of Cu- doped ZnO nanoparticle

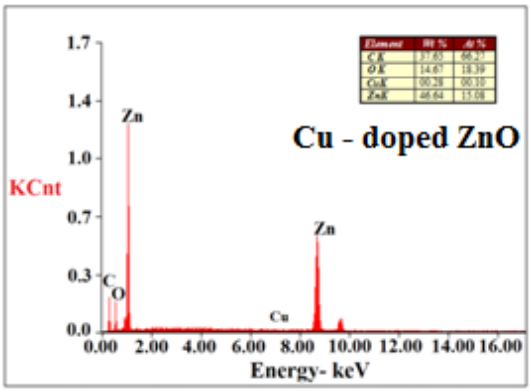

Fig. 3. EDX spectra of Cu- doped ZnO nanoparticle

3.2. Absorption and emission behaviour of MMPI with Cu -doped ZnO

The absorption spectra of MMPI in the presence and absence of nanoparticle are shown in figure 4. The nanoparticle enhances the absorbance of MMPI which indicates the nanocrystals do not adjust the excitation of the ligand. The enhanced absorption at 257 nm is due to adsorption of the MMPI on nanoparticle surface and effective electron transfer from the excited MMPI to the conduction band (CB) of the nanoparticle. Effect of increasing concentration of nanoparticle on the emission spectra is shown in figure 5. Adding of nanoparticle to MMPI resulted quenching of its emission [21].

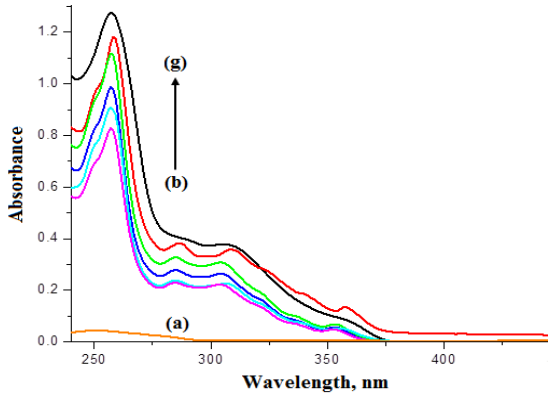

Fig. 4. Absorption spectra of MMPI in presence and absence of different concentration of (a) Bare, (b)–(g) MPMPI and Cu –doped ZnO 1x10^{-5}M to 4.5x10^{-5}M

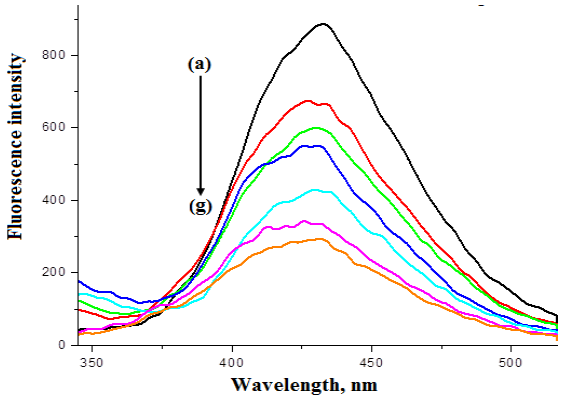

Fig. 5. Fluorescence spectra of MMPI in presence and absence of different concentration of (a) Bare, (b)–(g) MPMPI and Cu –doped ZnO 1x10^{-5}M to 4.5x10^{-5}M

3.3. HOMO and LUMO energy levels of MMPI and Cu -doped ZnO

From the onset oxidation potential (E_{ox}) and the onset reduction potential (E_{red}) of the derivative, HOMO and LUMO energy level have been calculated using the equations [22], HOMO = $-e(E_{ox} + 4.71)$ (eV); LUMO = $-e(E_{red} + 4.71)$ (eV). On the basis of the relative HOMO and LUMO energy level of an isolated MMPI molecule along with the conduction band and valence band edges of Cu –doped ZnO nanoparticle as shown in Figure 6, the electron injection would be thermodynamically allowed from the excited singlet of the MMPI derivative to the conduction band of Cu –doped ZnO.

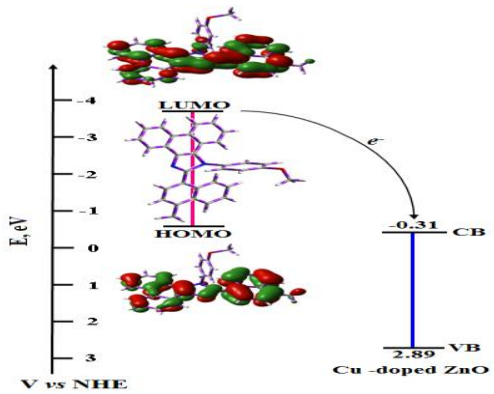

Fig. 6. HOMO and LUMO energy levels of MMPI along with the CB and VB edge of Cu-doped ZnO nanoparticle

4. Conclusions

Cu -doped ZnO nanoparticle prepared by sol-gel method and characterised by XRD, SEM, EDS, UV–visible spectroscopy and fluorescence spectra. The quenching process of MMPI is adsorbed on the surface of nanoparticle.

5. Acknowledgments

Instrumentation facility will be provided by Department of Physics (CSIL Lab), Annamalai University, Annamalainagar, is gratefully acknowledged. Dr. P. Ramanathan likes to thank the management of Thanthai Hans Roever College, Autonomous, Elambalur, Perambalur for the infrastructure and moral support.

References

1. A. Jaiswal, S.S. Ghosh, A. Chattopadhyay, Chem. Commun., Vol. 48, **(2012)**, pp. 407–409.
2. S. Reineke, F. Lindner, G. Schwartz, N. Seidler, K. Walzer, B. Luessem, K. Leo, Nature. Vol. 459, **(2009)**, pp. 234–238.
3. S.C. Vanithakumari, K.K. Nanda, Adv. Mater., vol. 21, **(2009)**, pp. 3581–3584.
4. F. Wang, Y.H. Chen, C.Y. Liu, D.G. Ma, Chem. Commun., vol. 47, **(2011)**, pp. 3502–3504.
5. K.S. Sanju, P.P. Neelakandan, D. Ramaiah, Chem. Commun., vol. 47, **(2011)**, pp. 1288–1290.
6. V. Vohra, G. Calzaferri, S. Destri, M. Pasini, W. Porzio, C. Botta, ACS Nano., vol. 4, (2010), pp. 1409–1416.
7. X. Wang, W. Li, K. Sun, J. Mater. Chem., vol. 21, **(2011)**, pp. 8558–8565.
8. K. Vanheusden, C.H. Seager, W.L. Warren, D. R. Tallant, J.A. Voigt, Appl. Phys. Lett., vol. 68, **(2008)**, pp. 403–405.
9. A. van Dijken, E.A. Meulenkamp, D. Vanmaekelbergh, J. Phys. Chem. B., vol. 104, **(2000)**, pp. 4355–4360.

10. H.J. Johnston, G.R. Hutchison, F.M. Christensen, S. Peters, S. Ankin, V. Stone, Part –I, Fibre Toxicol., 6, **(2009)**.
11. S. Sakohapa, L.D. Tickazen, M.A. Anderson, J. Phys. Chem., vol. 96, **(1992)**, pp. 11086.
12. K. Harada, K. Asakura, Y. Ueki, N. Toshina, J. Phys. Chem., vol. 96, **(1992)**, 9730.
13. J. Lee, J.H. Hwang, T.T. Mashek, T.O. Mason, A.E. Miller, R.W. Siegel, J. Mater. Res., vol. 10, **(1995)**, pp. 2295.
14. K. Hara, T. Horiguchi, T. Kinoshita, K. Sayama, H. Sugihara, H. Arakawa, Solar Energy Mater. Solar Cells., vol. 64, **(2000)**, pp. 115.
15. H. Cao, Jy. Xu, D.Z. Zhang, Phys. Rev. Lett., vol. 84, **(2000)**, pp. 5584.
16. D.M. Bagnall, Y.F. Chen, M.Y. Shen, Z. Zhu, T. Goto, T.J. Yao, Cryst. Growth, 605, **(1998)**, 184–185.
17. H.M. Xiong, Z.D. Wang, Y.Y. Xia, Adv. Mater., vol. 18, **(2006)**, pp. 748–751.
18. H.M. Xiong, Y. Xu, Q.G. Ren and Y.Y. Xia, J. Am. Chem. Soc., vol. 130, **(2008)**, pp. 7522–7523.
19. V. Subramanian, E.E. Wolf, P.V. Kamat, J. Phys. Chem. B., vol. 107, **(2003)**, pp. 7479–7485.
20. M. J. Frisch, G. W. Trucks, H. B. Schlegel, G. E. Scuseria, M. A. Robb, J. R. Cheeseman, J. A. Montgomery, Jr., T. Vreven, K. N. Kudin, J. C. Burant, J. M. Millam, S. S. Iyengar, J. Tomasi, V. Barone, B. Mennucci, M. Cossi, G. Scalmani, N. Rega, G. A. Petersson, H. Nakatsuji, M. Hada, M. Ehara, K. Toyota, R. Fukuda, J. Hasegawa, M. Ishida, T. Nakajima, Y. Honda, O. Kitao, H. Nakai, M. Klene, X. Li, J. E. Knox, H. P. Hratchian, J. B. Cross, V. Bakken, C. Adamo, J. Jaramillo, R. Gomperts, R. E. Stratmann, O. Yazyev, A. J. Austin, R. Cammi, C. Pomelli, J. W. Ochterski, P. Y. Ayala, K. Morokuma, G. A. Voth, P. Salvador, J. J. Dannenberg, V. G. Zakrzewski, S. Dapprich, A. D. Daniels, M. C. Strain, O. Farkas, D. K. Malick, A. D. Rabuck, K. Raghavachari, J. B. Foresman, J. V. Ortiz, Q. Cui, A. G. Baboul, S. Clifford, J. Cioslowski, B. B. Stefanov, G. Liu, A. Liashenko, P. Piskorz, I. Komaromi, R. L. Martin, D. J. Fox, T. Keith, M. A. Al-Laham, C. Y. Peng, A. Nanayakkara, M. Challacombe, P. M. W. Gill, B. Johnson, W. Chen, M. W. Wong, C. Gonzalez, J. A. Pople, Gaussian 03 (Revision E.01), Gaussian, Inc., Wallingford, CT. **(2004)**.
21. C. Huber, K. Fähnrich, C. Krause, T. Werner, J. Photochem. Photobiol. A: Chem., vol. 128, **(1999)**, pp. 111-120.
23. W.Y. He, Y. Li, C. Xue , Z.D. Hu, X.G. Chen, F.L. Sheng, Bioorg. Med. Chem., vol. 13, **(2005)**, pp. 1837-1845.